CHAPTER 5

OBSERVER BASED NMPC FOR CSTRs

5.1 INTRODUCTION

In this chapter observer based NMPC design proposed in chapter 3 is applied to CSTRs and results are presented. Also, the efficacy of proposed NMPC scheme to control the process even at unstable operating point has been demonstrated.

5.2 CLOSED-LOOP SIMULATION STUDIES OF CSTR-I

In all the simulation runs, the process is simulated using the nonlinear first principles model (Refer Equations 4.1 and 4.2) and the true state variables are computed by solving the nonlinear differential equations using differential equation solver in Matlab 6.5. NMPC schemes for CSTR-I have been developed with the sampling time of 0.083 min, prediction horizon of $N_P = 5$, and control horizon of $N_c = 1$. The error weighting matrix and the controller weighting matrix used in the NMPC formulation are $W_E = 1e^4$ and $W_U = 0$. Since the input weighting matrix is chosen as zero, we have selected the control horizon equal to one so that input moves are not aggressive. The following constraints on the manipulated input (coolant flow rate) are imposed $95 < q_c < 108$. The constrained optimization algorithm has been solved using the optimization toolbox commands in Matlab 6.5.

5.2.1 Servo response of CSTR-I with fuzzy dynamic model based NMPC

In order to assess the tracking capability of the proposed NMPC formulation using the fuzzy dynamic model the set point variations as shown in Figure 5.1(a) have been introduced. From the response it can be inferred that, the NMPC formulation is able to maintain the reactor concentration at the setpoint. The variation in the controller output is presented in Figure 5.1(b).

In order to assess the effect of the prediction horizon, we have performed simulation studies for various values of prediction horizon. The closed loop responses to step changes in the setpoint and for various values of prediction horizon are shown in Figure 5.2. In all the simulation runs a control horizon of 1 is used. The setpoint tracking performances have been found to be almost same for all the values of prediction horizons. The ISE values of fuzzy dynamic model based NMPC for various values of prediction horizon are reported in Table 5.1.

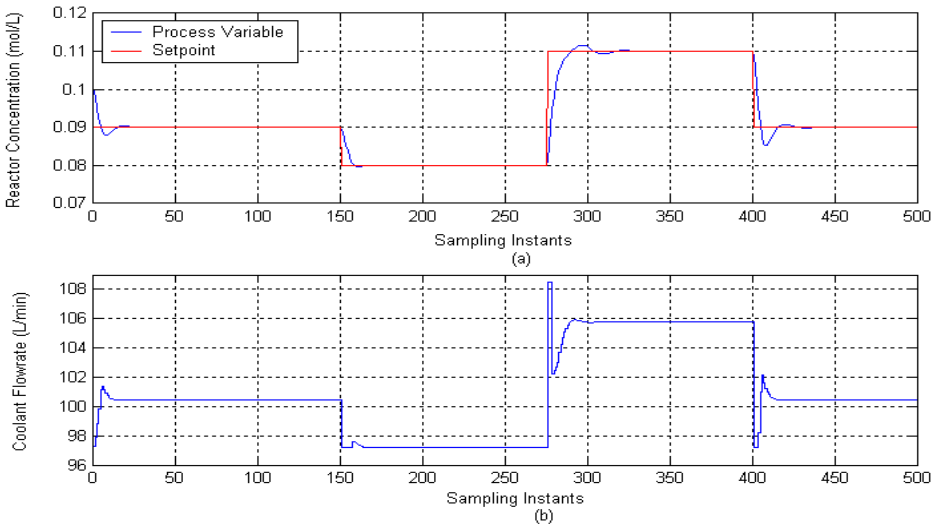

Figure 5.1 Servo response of CSTR-I with fuzzy dynamic model based NMPC (a) Process output (b) Controller output

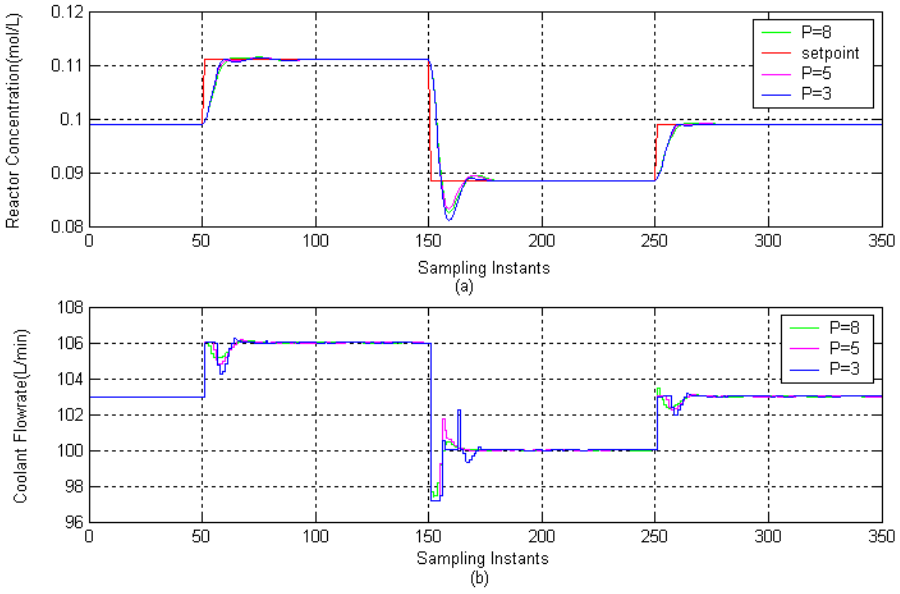

Figure 5.2 **Servo response of CSTR-I with fuzzy dynamic model based NMPC for various values of prediction horizon (a) Process output (b) Controller output**

Table 5.1 **ISE values of CSTR-I with fuzzy dynamic model based NMPC for various values of Prediction Horizon**

Sampling intervals	P = 3	P = 5	P = 8
1 - 150	$1.6025e^{-05}$	$1.6992e^{-05}$	$2.15151e^{-05}$
151 - 275	$9.9260e^{-04}$	$9.9353e^{-04}$	$9.9526e^{-04}$
276 - 400	0.0038	0.0039	0.0039
401 - 500	$1.0253e^{-04}$	$1.0528e^{-04}$	$1.1289e^{-04}$

5.2.2 Servo and regulatory responses of CSTR-I with fuzzy dynamic model based NMPC

Simulation study has been performed to assess the disturbance rejection capability of the proposed fuzzy dynamic model based NMPC at the nominal and shifted operating points. A step change in the feed temperature of magnitude 2 degree Kelvin (from 350 degree Kelvin to 352 degree Kelvin) has been introduced at 275th sampling instants and the value has been maintained up to 500th sampling instants and then brought back to 350 degree Kelvin. (Refer Figure 5.4). The set point variations as shown in Figure 5.3(a) have been introduced. The process output and the manipulated profile are shown in Figures 5.3(a) and 5.3(b) respectively.

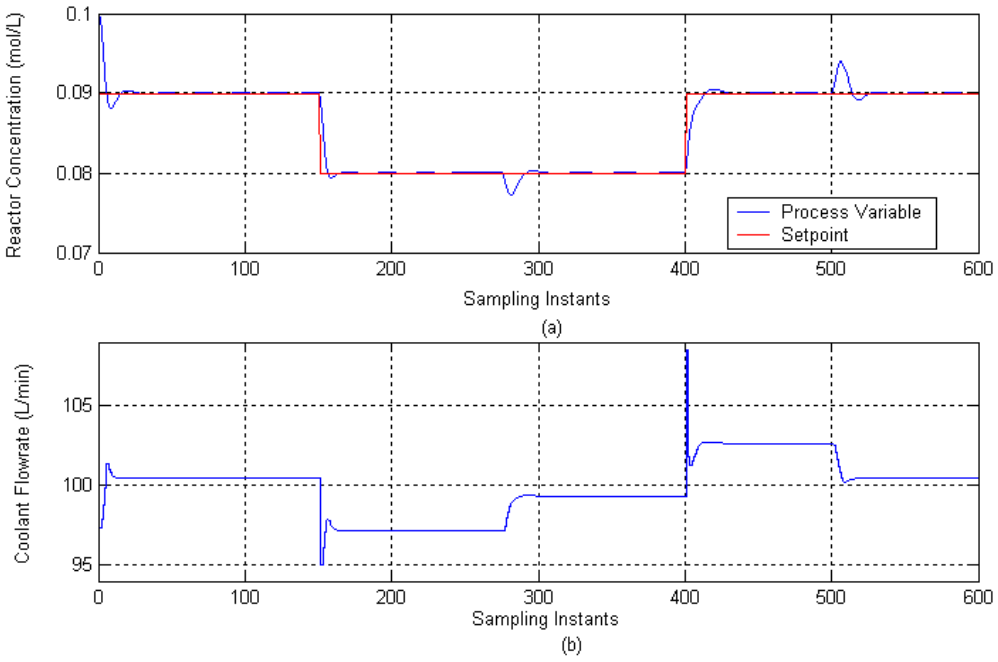

Figure 5.3 Servo and regulatory responses of CSTR-I with fuzzy dynamic model based NMPC (a) Process output (b) Controller output

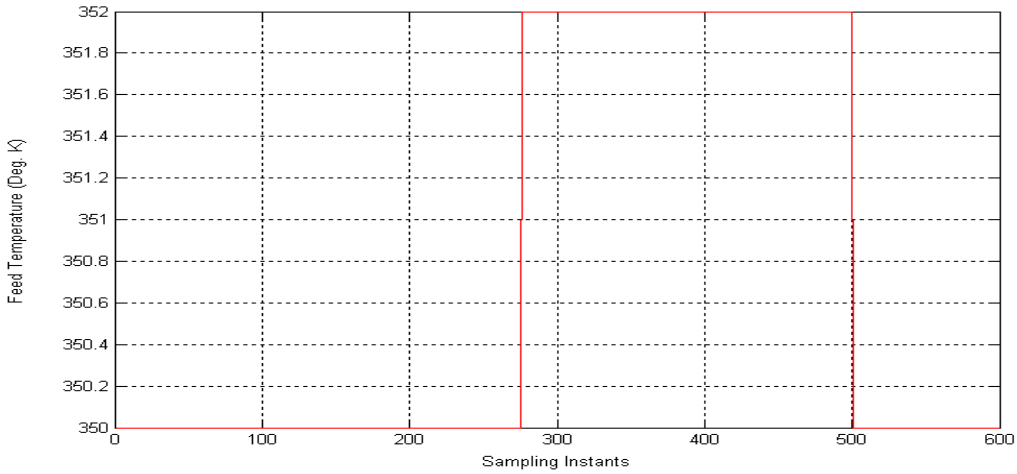

Figure 5.4 Variation in feed temperature of CSTR-I

5.2.3 Servo response of CSTR-I with FKF based NMPC

In order to assess the tracking capability of the proposed FKF based NMPC scheme a setpoint variation as shown in Figure 5.5(a) has been introduced. The state estimator used in the MPC is a fuzzy Kalman filter. We have assumed that the random errors are present in the measurements (C_A and T) as well as in the coolant flow rate (q_c). The covariance matrices of measurement noise and state noise are assumed as

$$R = \begin{bmatrix} (0.0025)^2 & 0 \\ 0 & (0.05)^2 \end{bmatrix} \quad \text{and} \quad Q = \begin{bmatrix} (0.05)^2 \end{bmatrix}$$

The initial value of the error covariance matrix $P(0/0)$ is assumed to be

$$P(0/0) = \begin{pmatrix} (0.05)^2 & 0 \\ 0 & (0.05)^2 \end{pmatrix}$$

From Figure 5.5(a), it is inferred that FKF based NMPC formulation was able to track the setpoint variations effectively. For the case of setpoint tracking we observed that the estimated states and true state are found to be close (Refer Figures 5.6 and 5.7). The controller output is shown in Figure 5.5(b).

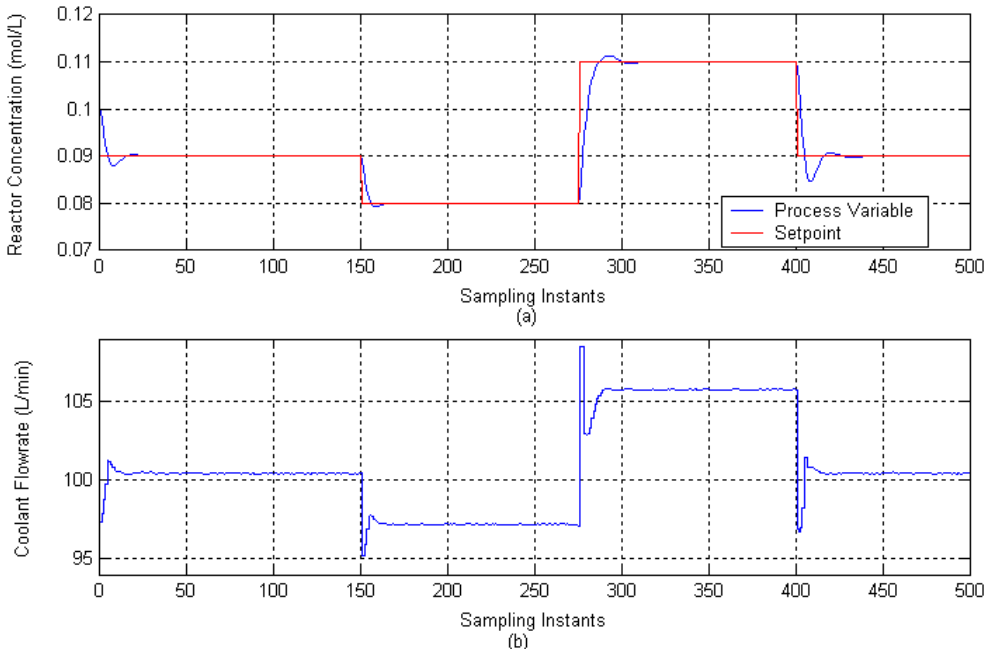

Figure 5.5 Servo response of CSTR-I with FKF based NMPC (a) Process output (b) Controller output

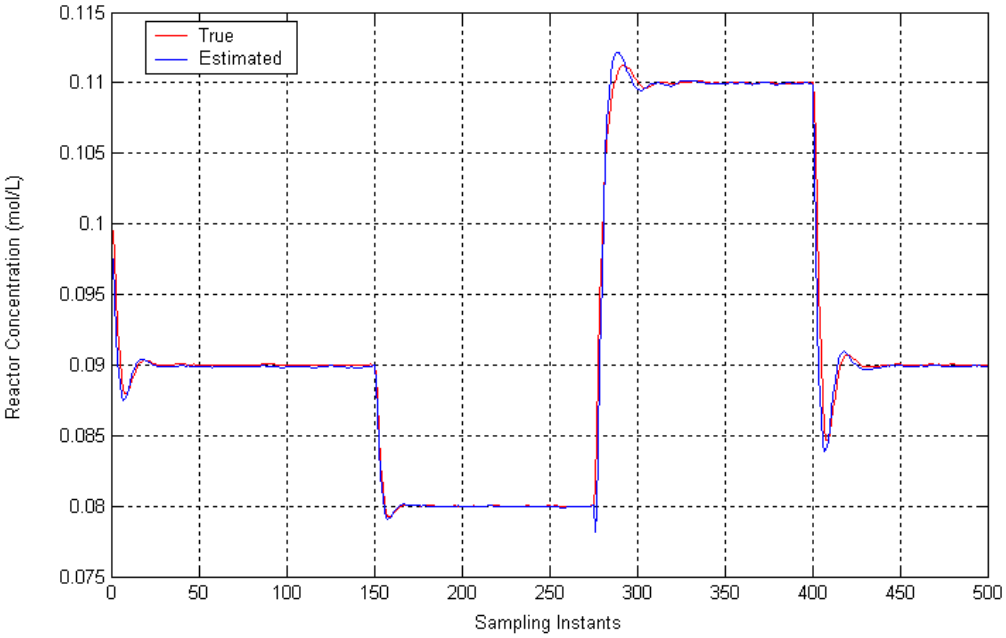

Figure 5.6 Evolution of true and estimated states of reactor concentration of CSTR-I with FKF based NMPC

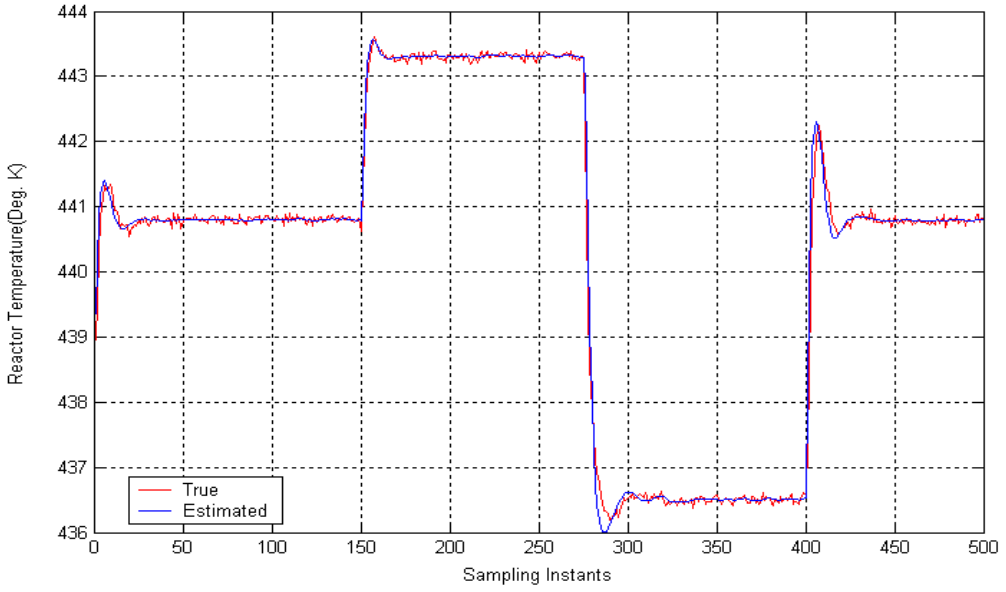

Figure 5.7 Evolution of true and estimated states of reactor temperature of CSTR-I with FKF based NMPC

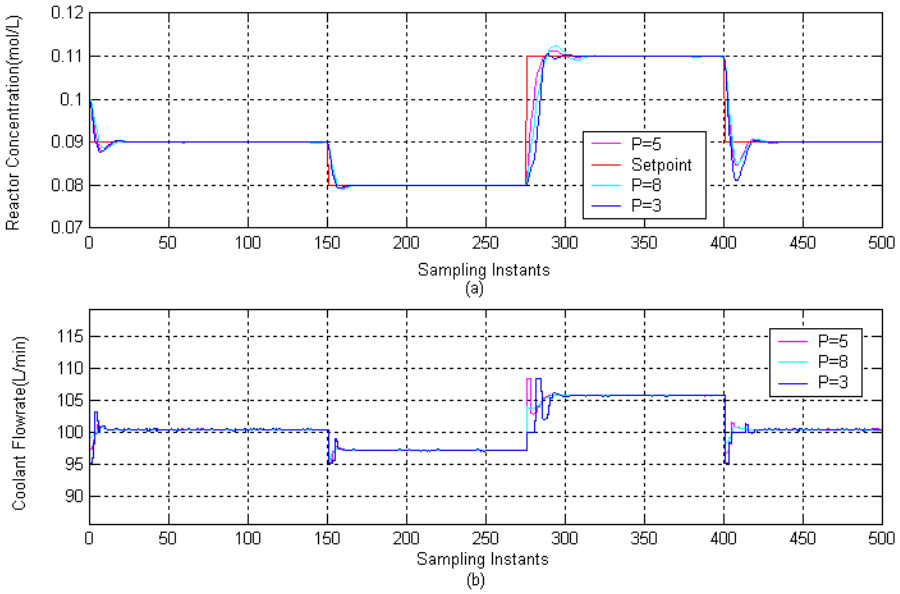

Figure 5.8 Servo response of CSTR-I with FKF based NMPC for various values of prediction horizon (a) Process output (b) Controller output

Table 5.2 ISE values of CSTR-I with FKF based NMPC for various values of prediction horizon

Sampling intervals	P = 3	P = 5	P = 8
1 – 150	$1.3915e^{-5}$	$1.7202e^{-5}$	$2.0183e^{-5}$
151 – 275	0.0010	0.0010	0.0010
276 – 400	0.0039	0.0040	0.0039
401 – 500	$1.2552e^{-4}$	$1.0654e^{-4}$	$1.1503e^{-4}$

The closed loop responses to step changes in the setpoint and for various values of prediction horizon are shown in Figure 5.8 and the ISE values of FKF based NMPC for various values of prediction horizon are reported in Table 5.2.

5.2.4 Regulatory response of CSTR-I with FKF based NMPC

The closed loop response to a step change in the feed temperature (Refer Figure 5.12) with FKF based NMPC is shown Figure 5.9(a). From the response, it can be concluded that FKF based NMPC is able to reject the disturbance and maintain the process variable at the desired setpoint. Figure 5.9(b) shows manipulated input profile of FKF based NMPC. We observed that the offset removal is at the cost of considerable bias in the estimated states of concentration and temperature (Refer Figures 5.10 and 5.11)

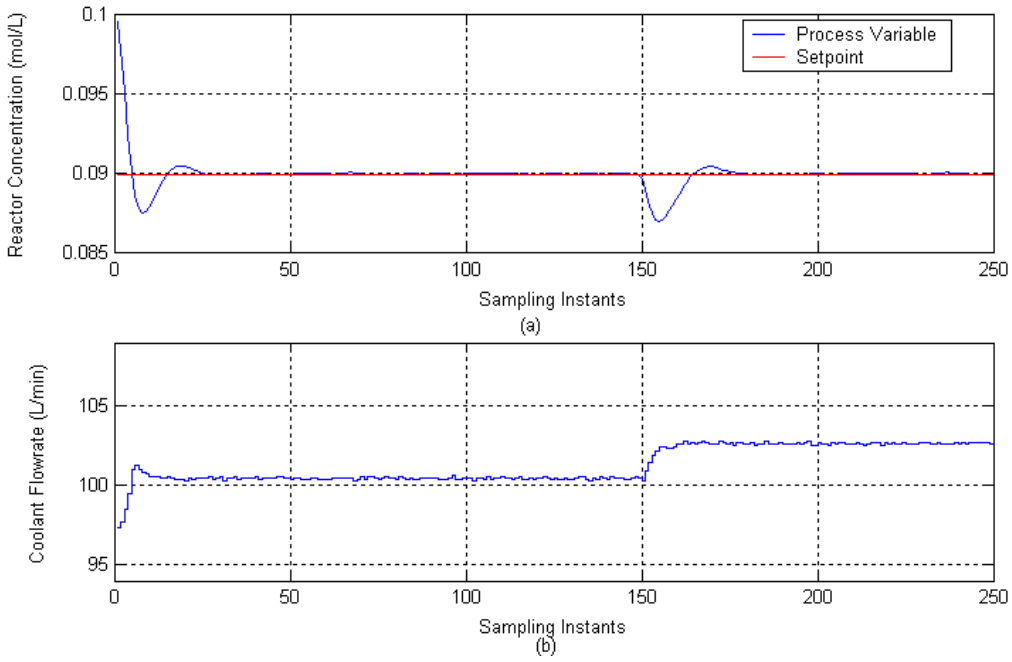

Figure 5.9 Regulatory response of CSTR-I with FKF based NMPC (a) Process output (b) Controller output

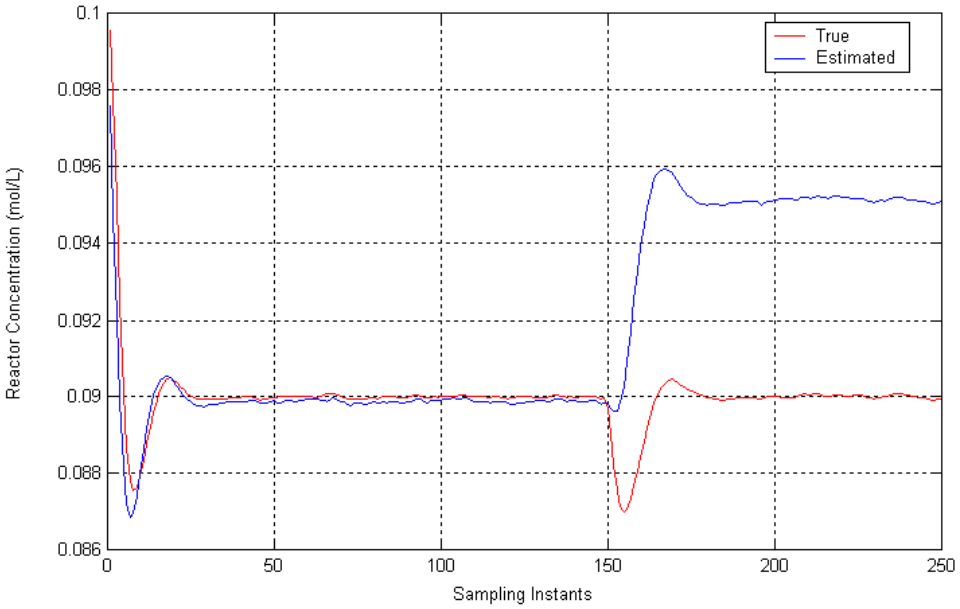

Figure 5.10 Evolution of true and estimated states of reactor concentration of CSTR-I in the presence of step change in feed temperature (FKF based NMPC)

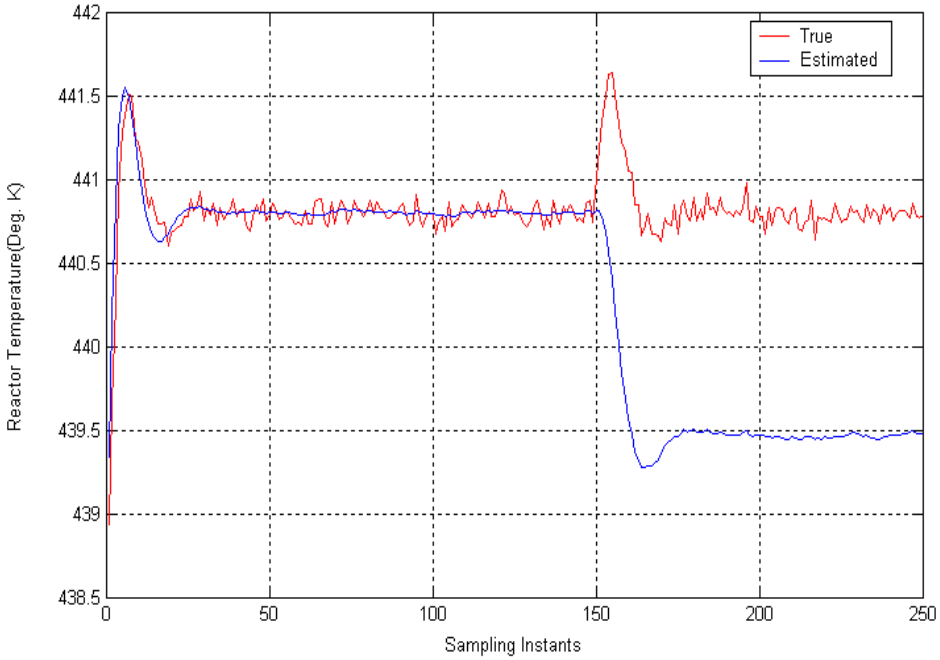

Figure 5.11 Evolution of true and estimated states of reactor temperature of CSTR-I in the presence of step change in feed temperature (FKF based NMPC)

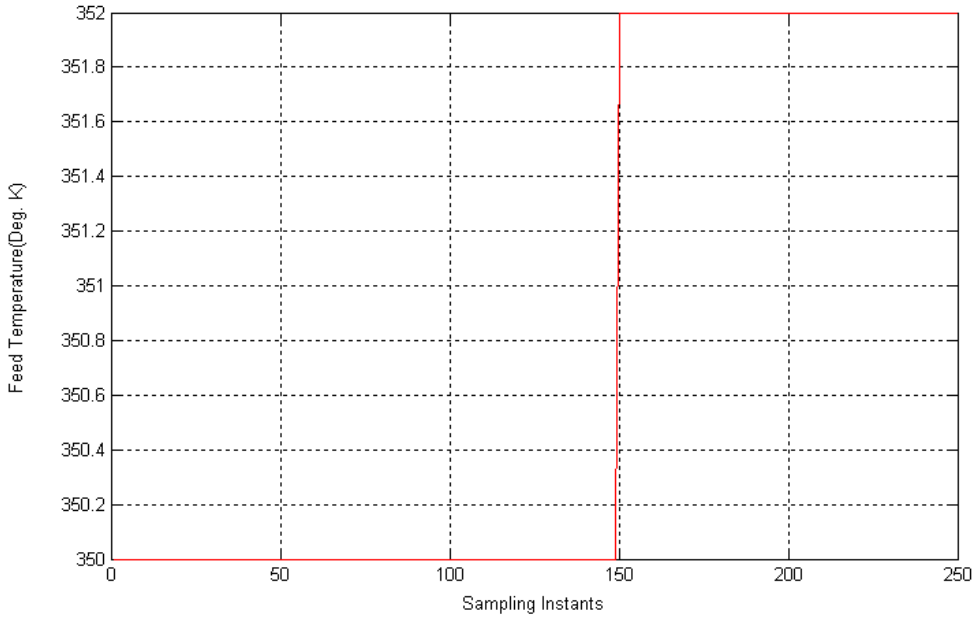

Figure 5.12 Variation in feed temperature of CSTR-I

5.2.5 Regulatory response of CSTR-I with ASFKF based NMPC

Simulation study has been performed to assess the disturbance rejection capability of the proposed ASFKF based NMPC at the nominal operating point. By considering the feed temperature as an additional state (unmeasured) variable and augmenting the state space model, an augmented state fuzzy Kalman filter has been used as a state estimator in the MPC. The noise covariance matrix Q_β is assumed to be 6.25×10^{-2}. The initial value of the additional state variable is chosen to be equal to the nominal steady-state value. The closed loop response of the ASFKF based NMPC in the presence of step change in the feed temperature (Refer Figure 5.16) is shown in Figure 5.13(a). The controller output profile is shown in Figure 5.13(b). It should be noted that in the case of ASFKF based NMPC the estimated states and true state are found to be close (Refer Figures 5.14 and 5.15).

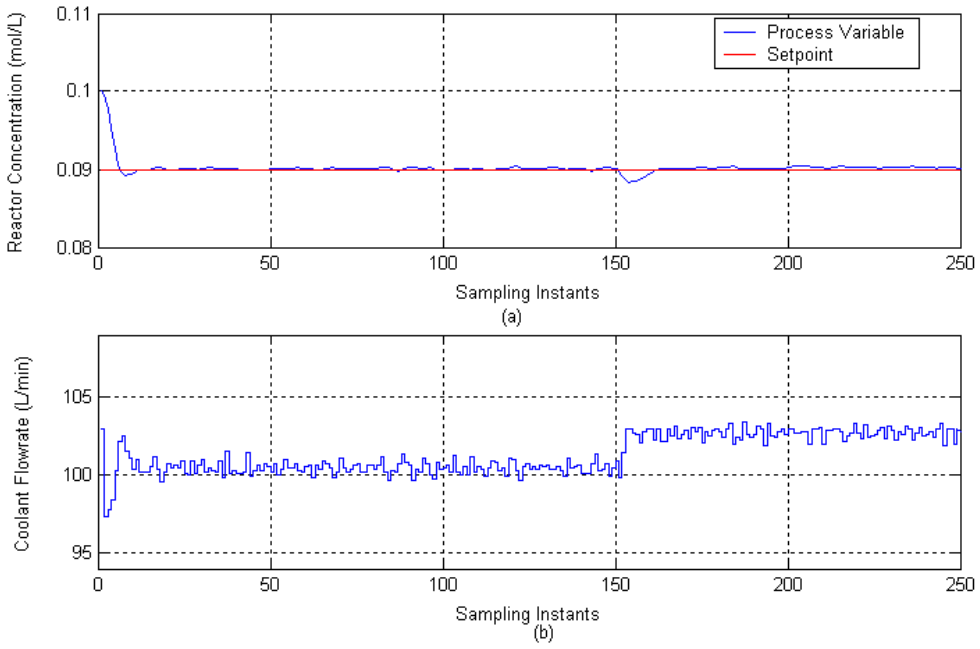

Figure 5.13 Regulatory response of CSTR-I with ASFKF based NMPC (a) Process output (b) Controller output

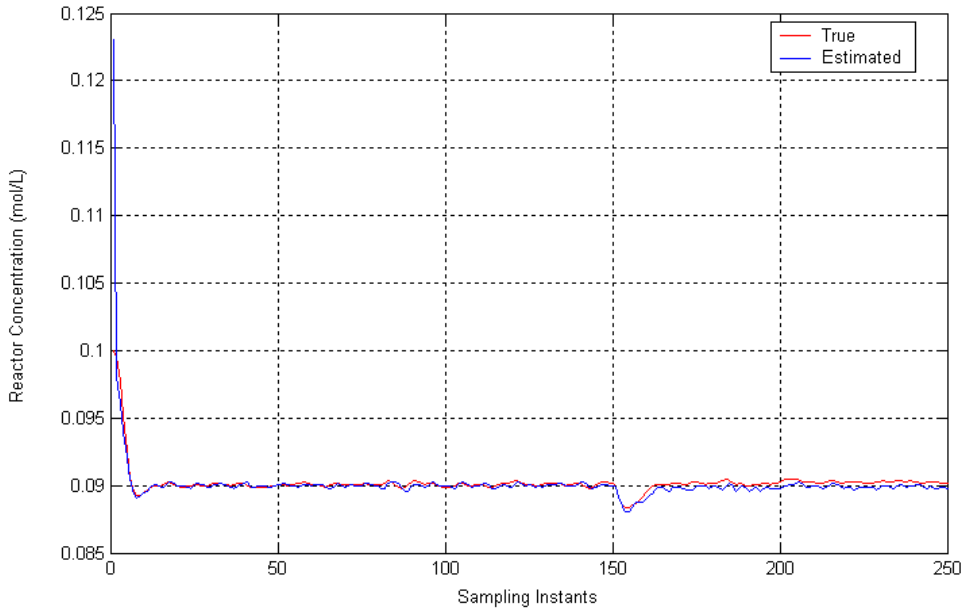

Figure 5.14 Evolution of true and estimated states of reactor concentration of CSTR-I in the presence of step change in feed temperature (ASFKF based NMPC)

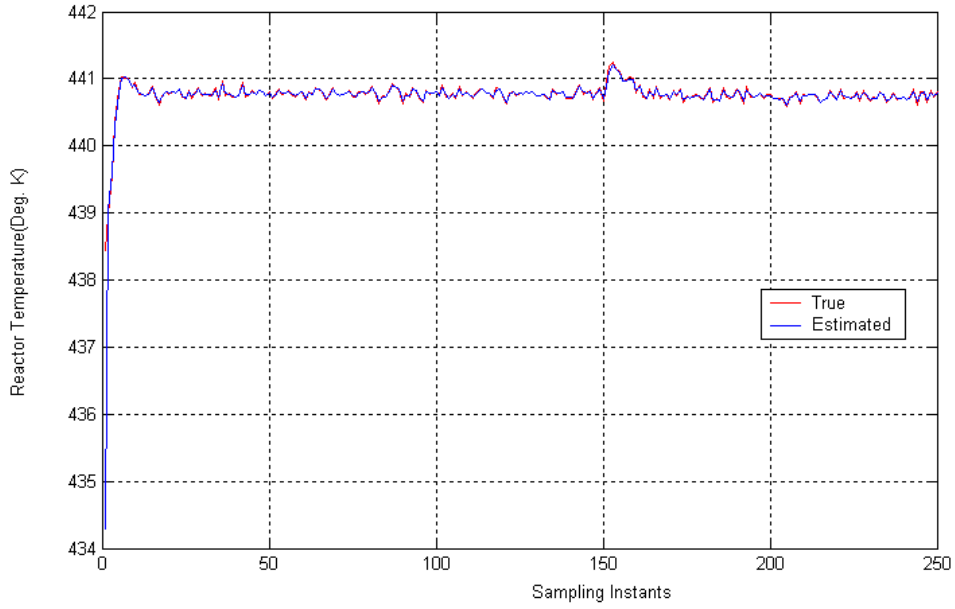

Figure 5.15 Evolution of true and estimated states of reactor temperature of CSTR-I in the presence of step change in feed temperature (ASFKF based NMPC)

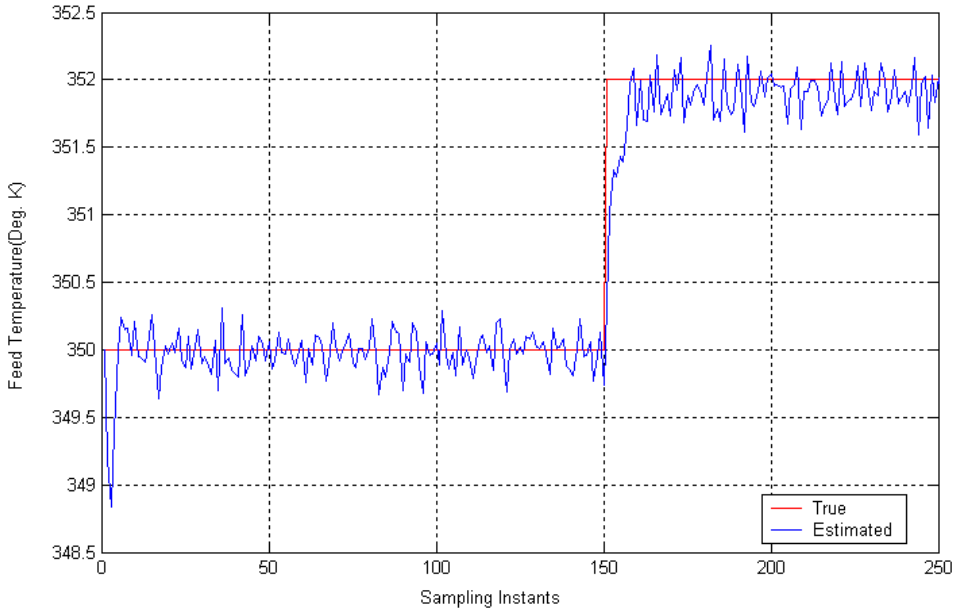

Figure 5.16 Evolution of true and estimated feed temperatures of CSTR-I (ASFKF based NMPC)

5.2.6 Servo response of CSTR-I with FKF based NMPC (Inferential Measurement)

We have simulated an inferential control case, where the reactor concentration is not measured, but estimated from temperature measurement and used in the FKF based NMPC formulation. For the inferential control case, we have assumed that the random errors are present in the measurement (T) as well as in the coolant flow rate (q_c). The covariance matrices of measurement noise and state noise are assumed as

$$R = \left[(0.05)^2 \right] \quad \& \quad Q = \left[(0.05)^2 \right]$$

The initial value of the error covariance matrix $P(0/0)$ is assumed to be

$$P(0/0) = \begin{pmatrix} (0.05)^2 & 0 \\ 0 & (0.05)^2 \end{pmatrix}$$

Figure 5.17 shows the closed loop response for the inferential control case. From the response (Refer Figure 5.17(a)) it is inferred that FKF was able to maintain the process variable (reactor concentration) at the desired setpoint even when reactor temperature alone is measurable. On the other hand there exist an offset between the true value of the process variable and the setpoint in the case of Linear Model Predictive Control scheme (LMPC). This is a consequence of the fact that the estimated concentration and temperature variables are biased (Figures 5.19) in the case of LMPC, whereas the state estimates generated by FKF are found to be fairly accurate. The true and estimated state variables for FKF based MPC and LMPC are shown in Figures 5.18 and 5.19.

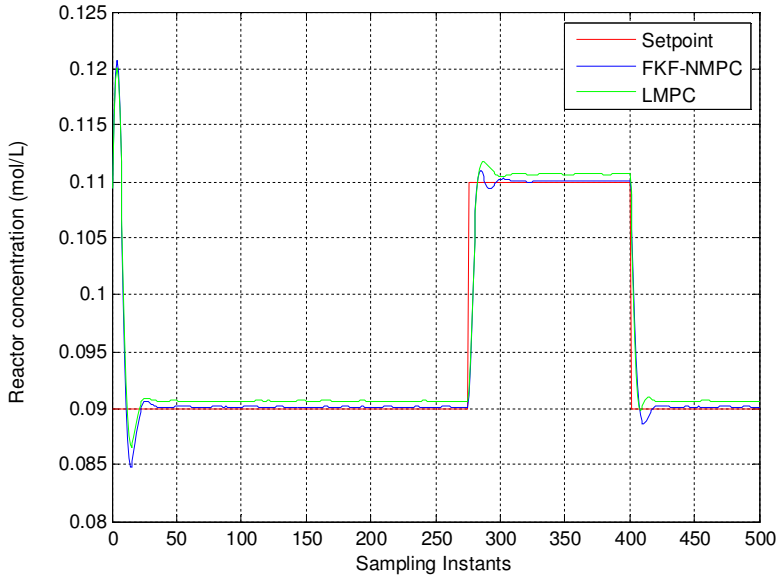

Figure 5.17 Servo response of CSTR-I (Inferential Control Case) (Process output)

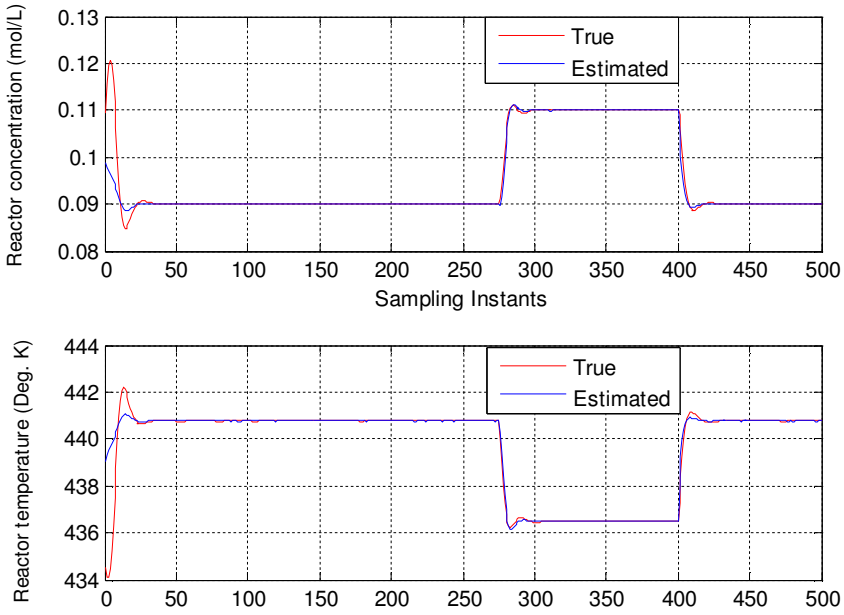

Figure 5.18 Evolution of true and estimated state variables of CSTR-I with FKF based NMPC (Inferential Control Case-Servo Problem)

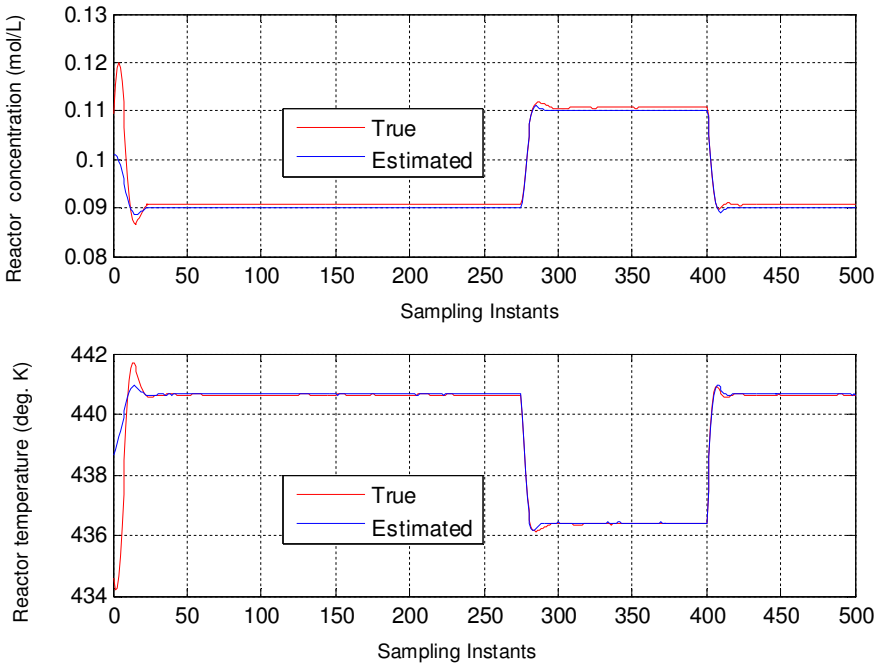

Figure 5.19 Evolution of true and estimated state variables with LMPC (Inferential Control Case-Servo Problem)

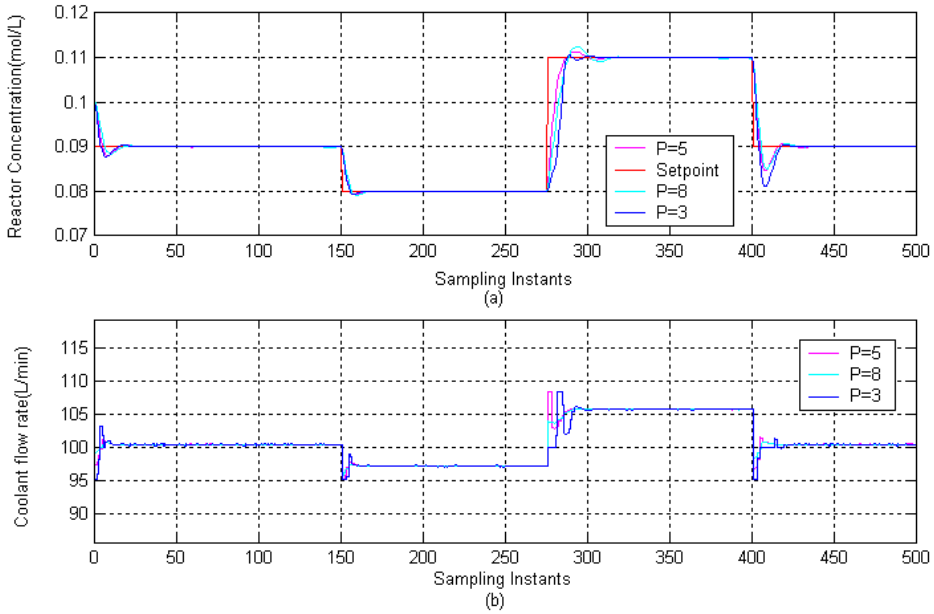

Figure 5.20 Servo response of CSTR-I for various values of prediction horizon with FKF based NMPC (Inferential Control Case) (a) Process output (b) Controller output

The closed loop responses to step changes in the setpoint and for various values of prediction horizon are shown in Figure 5.20 and the ISE values of FKF based NMPC (Inferential control case) for various values of prediction horizon are reported in Table 5.3.

Table 5.3 ISE values of CSTR-I with FKF based NMPC (Inferential Control Case) for various values of Prediction Horizon

Sampling intervals	P = 3	P = 5	P = 8
1 - 150	$1.2925e^{-05}$	$1.6428e^{-05}$	$1.9504e^{-05}$
151 - 275	0.0010	0.0010	0.0010
276 - 400	0.0039	0.0040	0.0040
401 - 500	$9.7291e^{-05}$	$9.535e^{-05}$	$1.0390e^{-04}$

5.2.7 Regulatory response of CSTR-I with FKF and ASKF based NMPC schemes (Inferential Measurement)

The closed loop performances of FKF and ASFKF based NMPC schemes when the reactor concentration is not measured, but estimated from temperature measurement and in the presence of step change in feed temperature (Refer Figure 5.28) are shown in Figures 5.21(a) and 5.25(a). Figure 5.21(a) show that FKF based NMPC results in an offset between the true concentration (inferred variable) and the setpoint. This is a consequence of the fact that the estimated concentration and temperature are biased (Figures 5.22 and 5.23) in the presence of step change in the feed temperature. The ASFKF formulation on the other hand is able to maintain the true concentration at the desired setpoint. This can be attributed to the fact that, unbiased state estimates are obtained in the case of ASFKF based state estimation approach (Refer Figures 5.26 and 5.27). The controller output of FKF and ASFKF are shown in Figures 5.21(b) and 5.25(b) respectively.

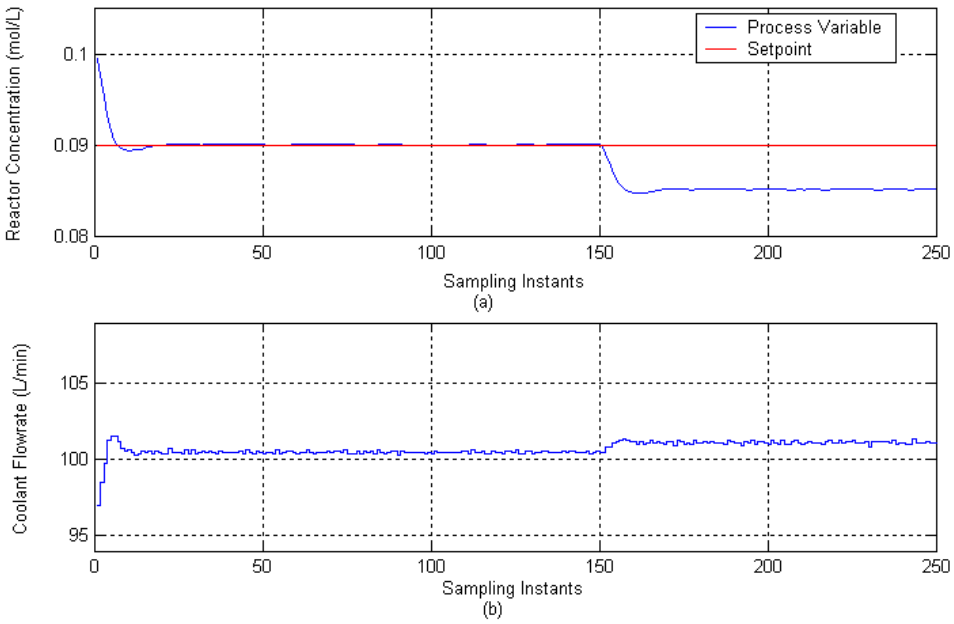

Figure 5.21 Regulatory response of CSTR-I with FKF based NMPC (Inferential Control Case) (a) Process output (b) Controller output

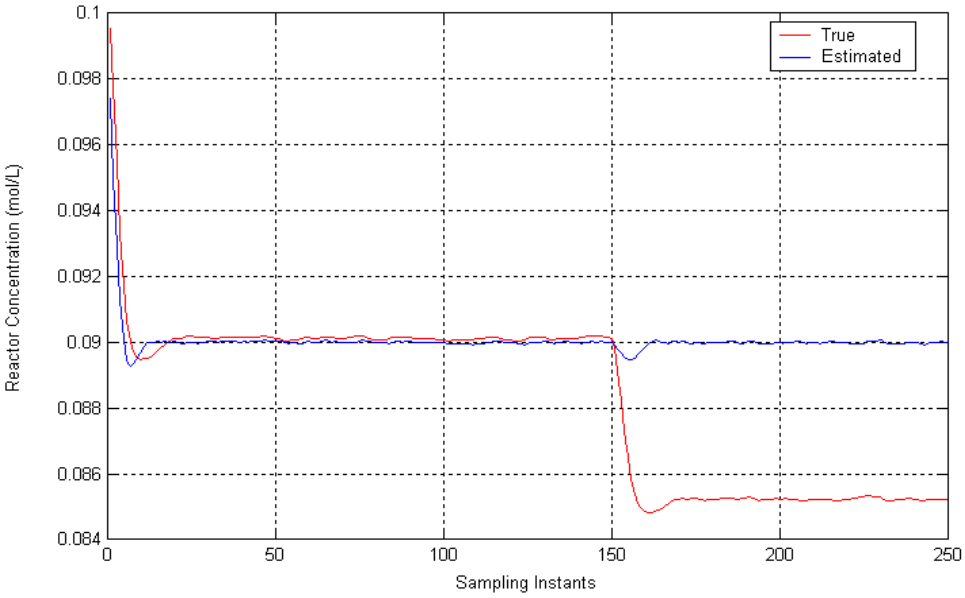

Figure 5.22 Evolution of true and estimated states of reactor concentration of CSTR-I in the presence of step change in feed temperature (FKF based NMPC - Inferential Control Case)

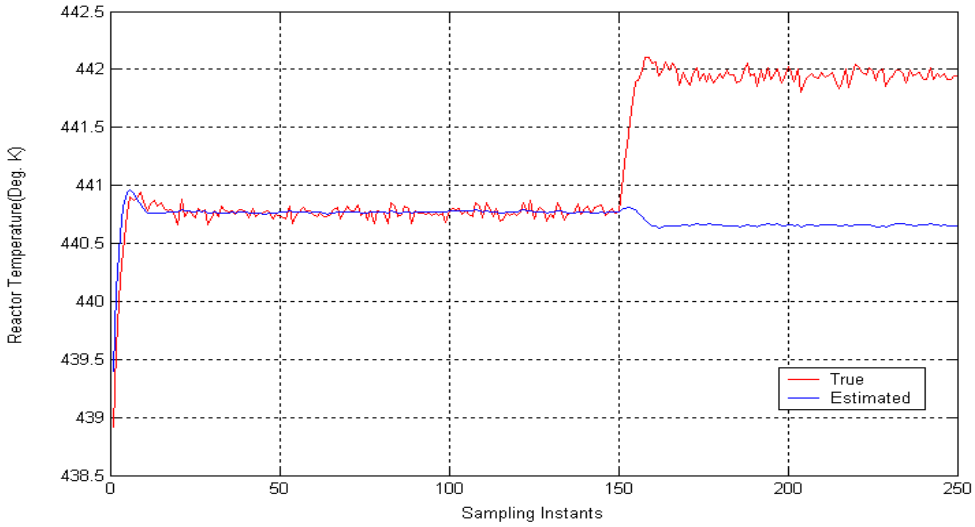

Figure 5.23 Evolution of true and estimated states of reactor temperature of CSTR-I in the presence of step change in feed temperature (FKF based NMPC-Inferential Control Case)

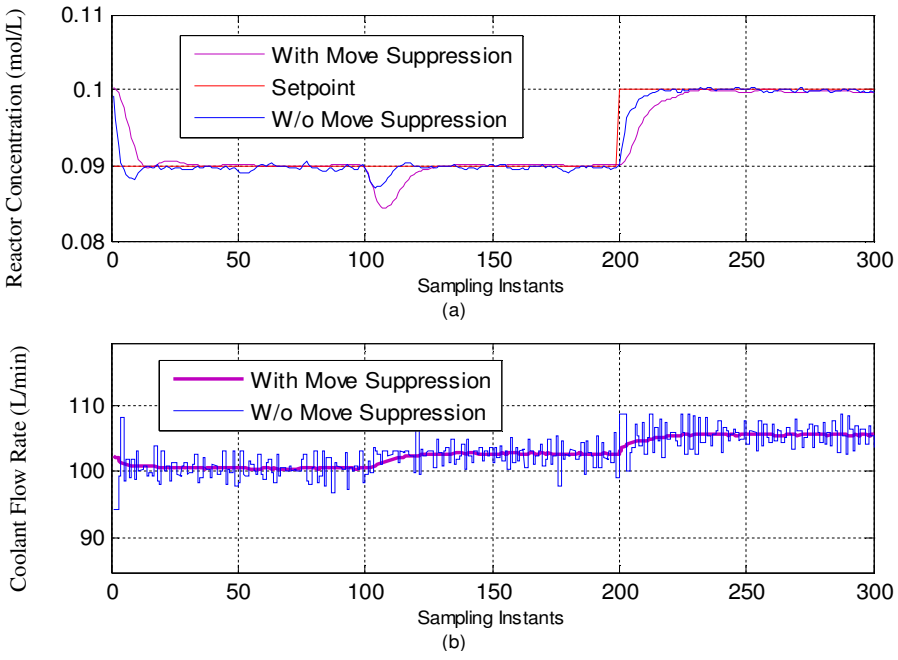

Figure 5.24 Servo-Regulatory response of CSTR with FKF based NMPC (with and without Move Suppressions) (a) Process output (b) Controller output

In order to suppress aggressive control action, move suppression has been applied on the manipulated variable and Figure 5.24(a) shows the servo-regulatory response with FKF based NMPC. Figure 5.24(b) shows manipulated input profile. For this application, the prediction horizon, control horizon and W_U have been chosen as 8, 2 and 2 respectively. It should be noted that a step change in the feed temperature of magnitude 2 degree Kelvin (from 350 degree Kelvin to 352 degree Kelvin) has been introduced at 100th sampling instants and the value has been maintained up to 300th sampling instants. With the disturbance being persistent, a step change in the setpoint has been introduced at 200th sampling instant (Refer Figure 5.24(a)). From Figure 5.24(a) it can be concluded that the controller is able to reject the disturbance as well as maintain the process variable at the setpoint.

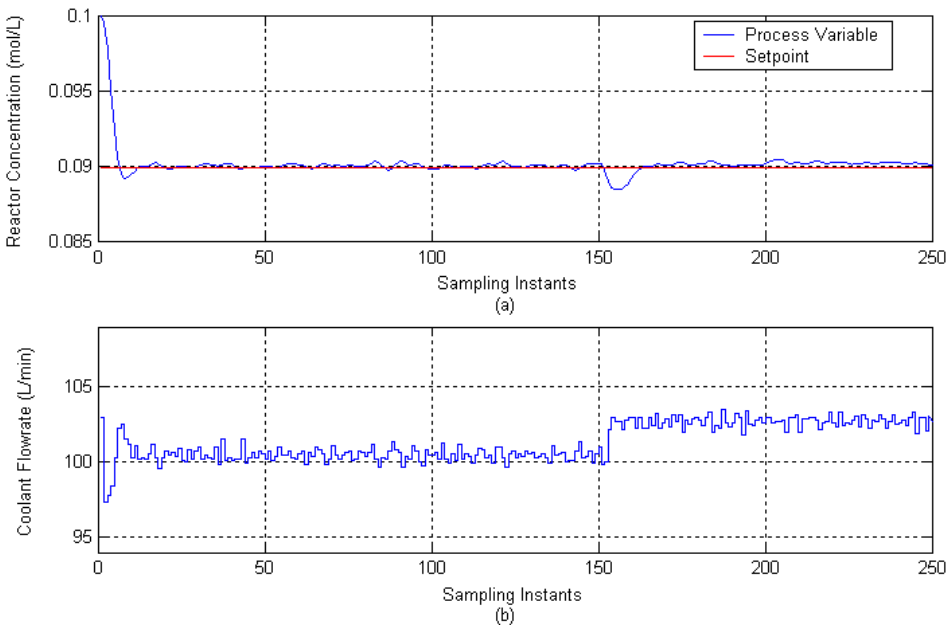

Figure 5.25 Regulatory response of CSTR-I with ASFKF based NMPC (Inferential Control Case) (a) Process output (b) Controller output

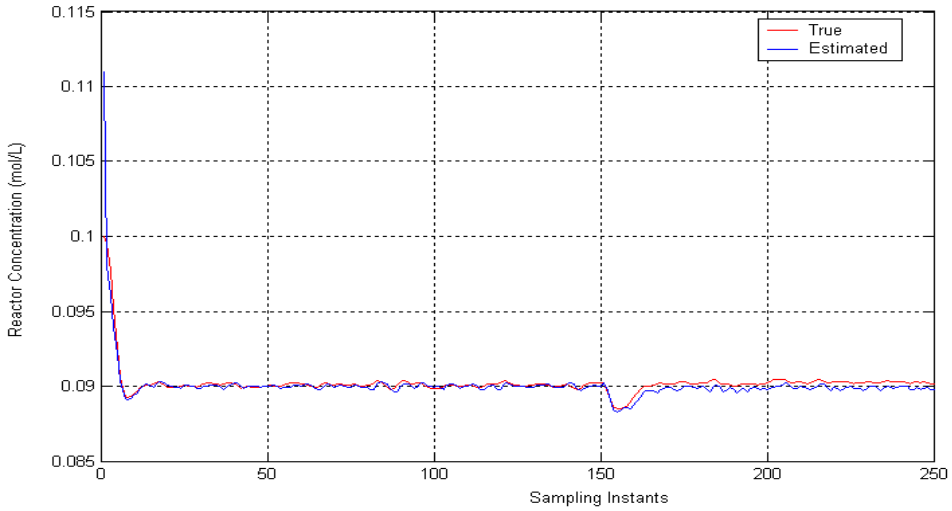

Figure 5.26 Evolution of true and estimated states of reactor concentration of CSTR-I in the presence of step change in feed temperature (ASFKF based NMPC-Inferential Control Case)

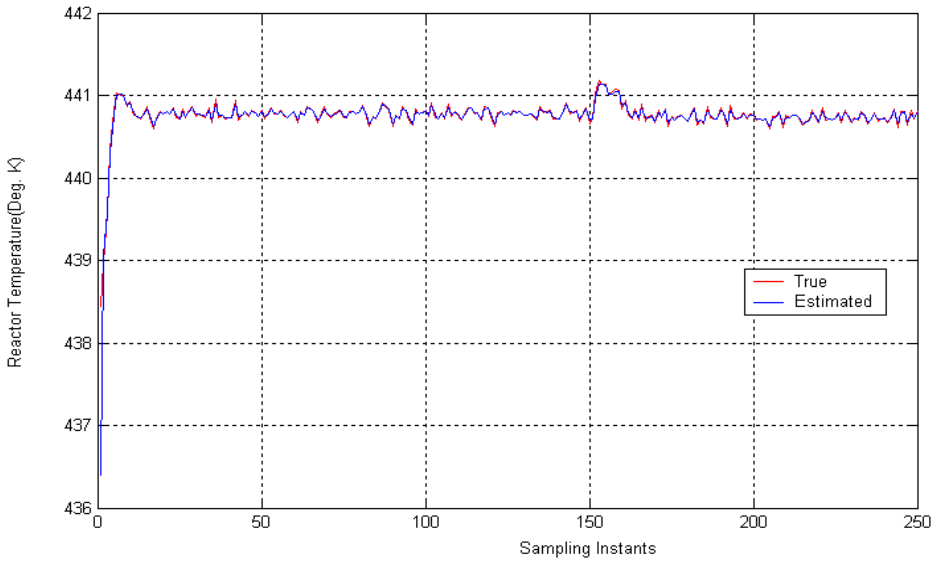

Figure 5.27 Evolution of true and estimated states of reactor temperature of CSTR-I in the presence of step change in feed temperature (ASFKF based NMPC-Inferential Control Case)

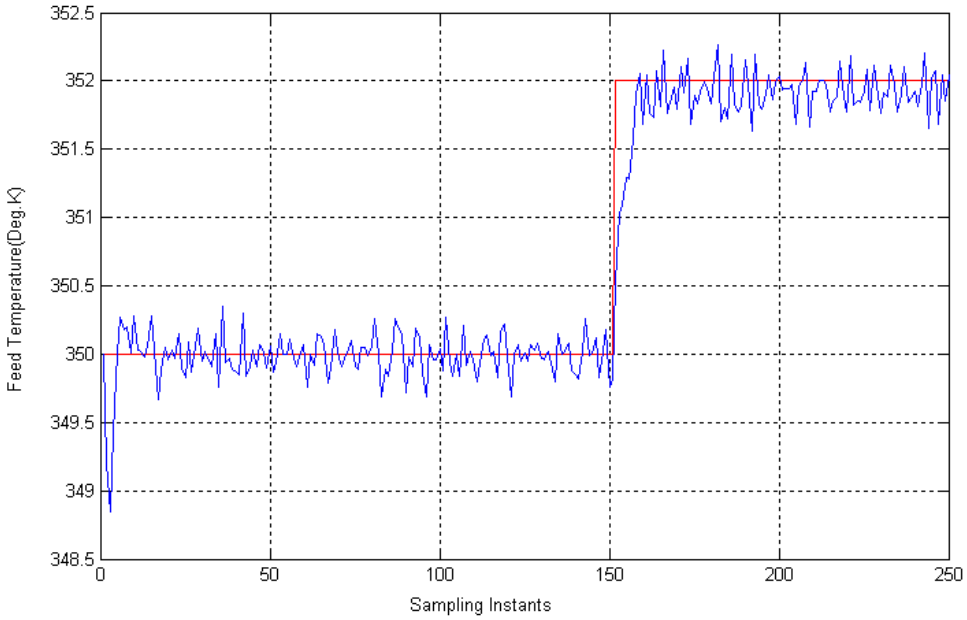

Figure 5.28 Evolution of true and estimated feed temperatures of CSTR-I (ASFKF based NMPC-Inferential Control Case)

5.3 CLOSED-LOOP SIMULATION STUDIES OF CSTR-II

In this section closed loop simulation studies have been carried out to demonstrate the efficacy of the proposed state estimation based NMPC scheme to control the process at unstable operating point. In all the simulation runs for CSTR-II, the process is simulated using the nonlinear first-principles model (Equations 4.5 and 4.6) and the true state variables are computed by solving the nonlinear differential equations Bequette (2002 and 2003) using the differential equation solver in Matlab 6.5. In all the simulation runs of the CSTR-II, we have assumed that the random errors are present in the measurements (C_A and T) as well as in the jacket temperature. The covariance matrices of measurement noise and state noise are assumed as:

$$R = \begin{bmatrix} (0.0025)^2 & 0 \\ 0 & (0.05)^2 \end{bmatrix} \quad Q = \begin{bmatrix} (0.05)^2 \end{bmatrix}$$

The initial value of the error covariance matrix $P(0/0)$ is assumed to be

$$P(0/0) = \begin{pmatrix} (0.05)^2 & 0 \\ 0 & (0.05)^2 \end{pmatrix}$$

NMPC schemes for CSTR-II have been developed with the sampling time of 0.1 hr, prediction horizon of $N_P = 5$, and control horizon of $N_c = 1$. The error weighting matrix and the controller weighting matrix used in the NMPC formulation are $W_E = 1$ and $W_U = 0$. Since the input weighting matrix is chosen as zero, we have selected the control horizon equal to one so that input moves are not aggressive. The following constraints on the manipulated input (jacket temperature) are imposed $280 < T_j < 320$.

5.3.1 Servo response of CSTR-II with FKF based NMPC

In order to assess the tracking capability of the proposed FKF based NMPC scheme a setpoint variation as shown in Figure 5.29a has been introduced. The state estimator used in the MPC is a fuzzy Kalman filter. The FKF will provide to the NMPC the estimated value of the states (concentration and temperature) of the nonlinear process (CSTR-II). The servo response is shown in Figure 5.29(a). The corresponding manipulated input profile and the evolution of true and estimated states are shown in Figures 5.29(b), 5.30 and 5.31 respectively. From the response it can be concluded that the NMPC scheme is found to achieve a smooth transition for large magnitude set point change (That is from stable operating point to unstable operating point).

In order to assess the effect of the prediction horizon, we have performed simulation studies for various values of prediction horizon. The closed loop responses to step changes in the setpoint and for various values of prediction horizon are shown in Figure 5.32. In all the simulation runs a control horizon of 1 is used. The setpoint tracking performances have been found to be the same for all the values of prediction horizon. The ISE values of FKF based NMPC for various values of prediction horizon are reported in Table 5.4.

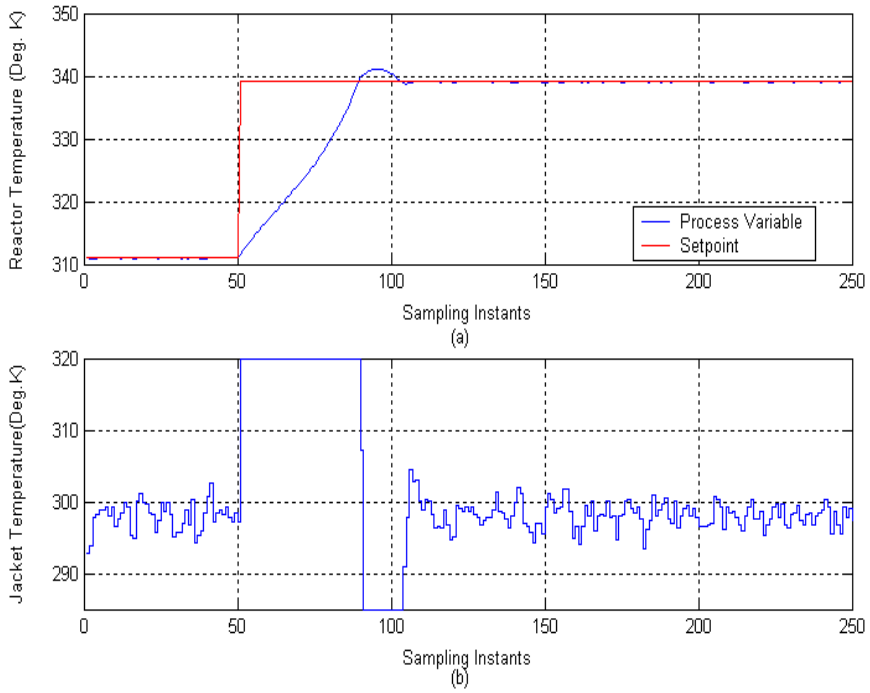

Figure 5.29 Servo response of CSTR-II with FKF based NMPC (a) Process output (b) Controller output

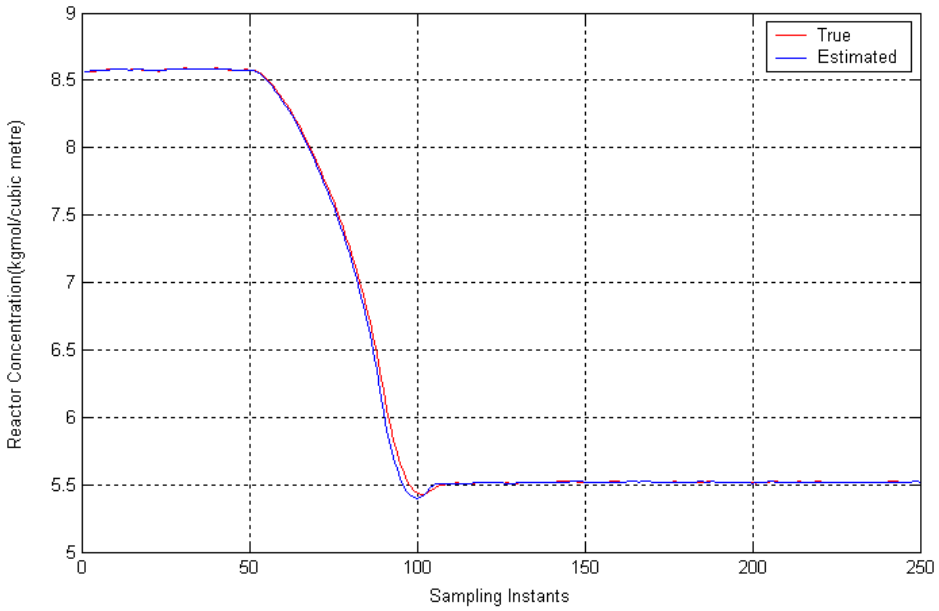

Figure 5.30 Evolution of true and estimated states of reactor concentration of CSTR-II with FKF based NMPC

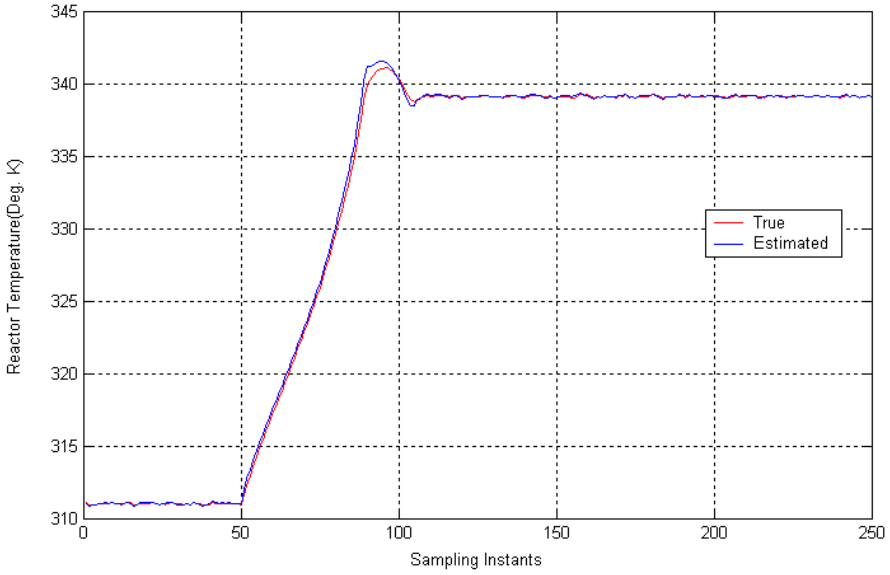

Figure 5.31 Evolution of true and estimated states of reactor temperature of CSTR-II with FKF based NMPC

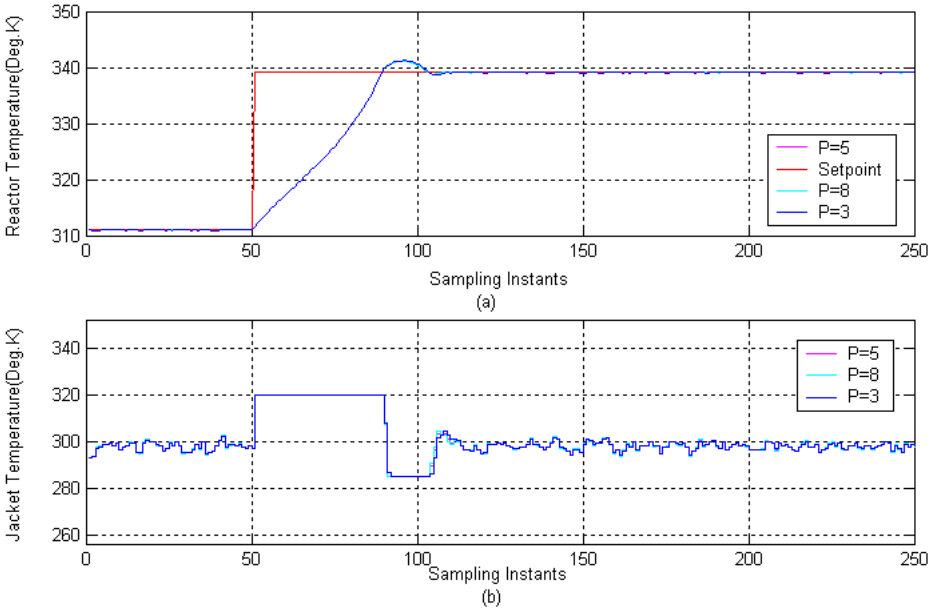

Figure 5.32 Servo response of CSTR-II with FKF based NMPC for various values of prediction horizon (a) Process output (b) Controller output

Table 5.4 ISE values of CSTR-II with FKF based NMPC for various values of prediction horizon

Sampling intervals	P = 3	P = 5	P = 8
1 – 50	0.0187	0.0187	0.0187
51 – 250	$1.1672e^{03}$	$1.1673e^{03}$	$1.1678e^{03}$

5.3.2 Regulatory response of CSTR-II with FKF and ASKF based NMPC schemes

The closed loop performances of FKF and ASFKF based NMPC schemes in the presence of step change in feed temperature (Refer Figure 5.36) are shown in Figures 5.33(a) and 5.37(a). It should be noted that fairly accurate state estimates (Refer Figures 5.38 and 5.39) are obtained in the case ASFKF based state estimation. This can be attributed to the fact that the unmeasured disturbance (feed temperature) is also estimated along with the reactor concentration and reactor temperature in the case of ASFKF. On the other hand estimated concentration and temperature are biased (Refer Figures 5.34 and 5.35) in the presence of step change in the feed temperature in the case of FKF based NMPC. The manipulated profiles of FKF and ASFKF based NMPC schemes are shown in Figures 5.33(b) and 5.37(b) respectively. From this simulation it can be concluded that the FKF and ASFKF based NMPC schemes are able to reject the disturbance and maintain the reactor temperature at 339.1 Deg. K. The evolution of true and estimated feed temperatures are shown in Figure 5.40.

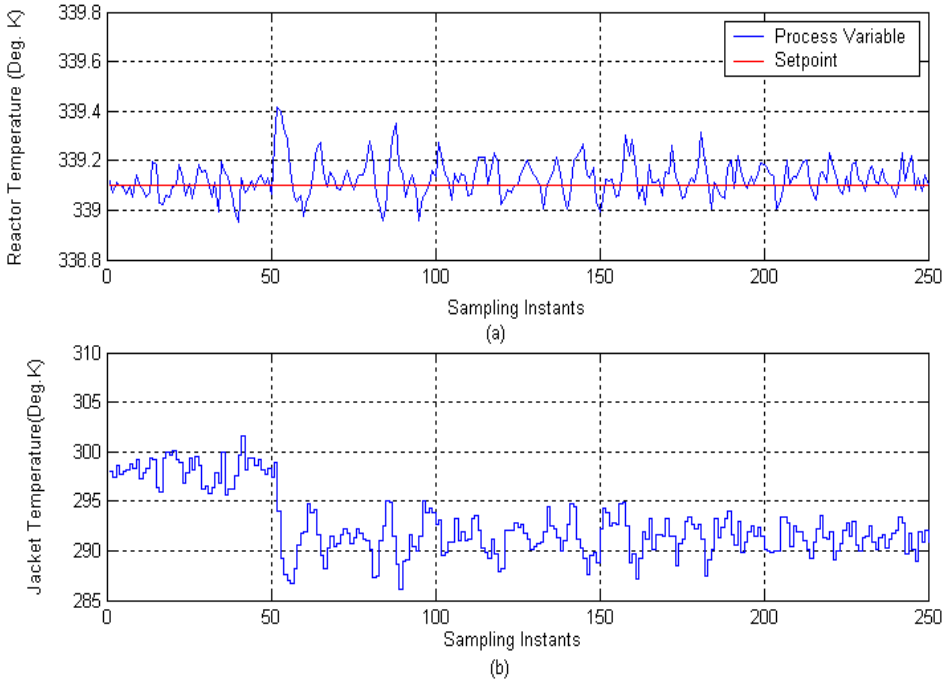

Figure 5.33 Regulatory response of CSTR-II with FKF based NMPC (a) Process output (b) Controller output

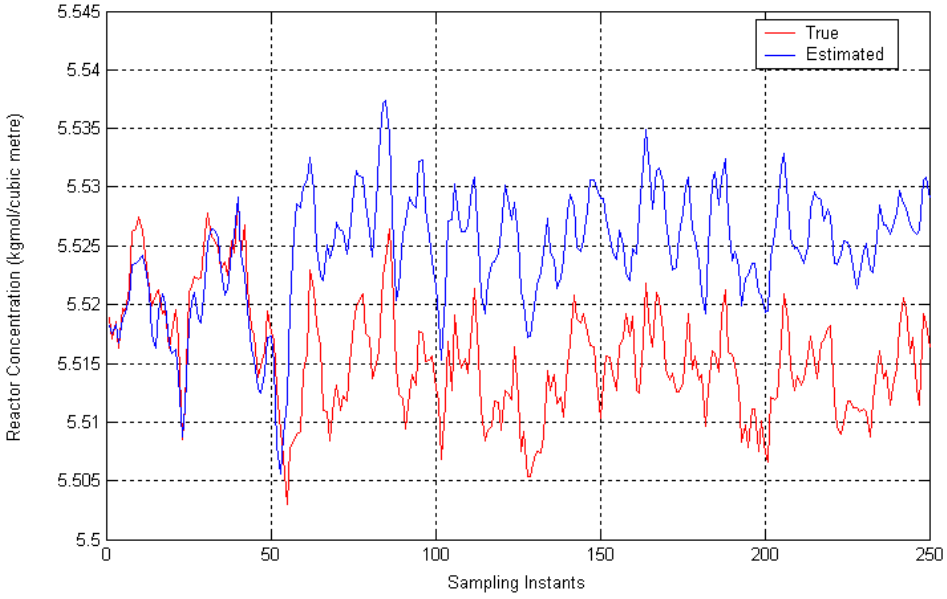

Figure 5.34 Evolution of true and estimated states of reactor concentration of CSTR-II in the presence of step change in feed temperature (FKF based NMPC)

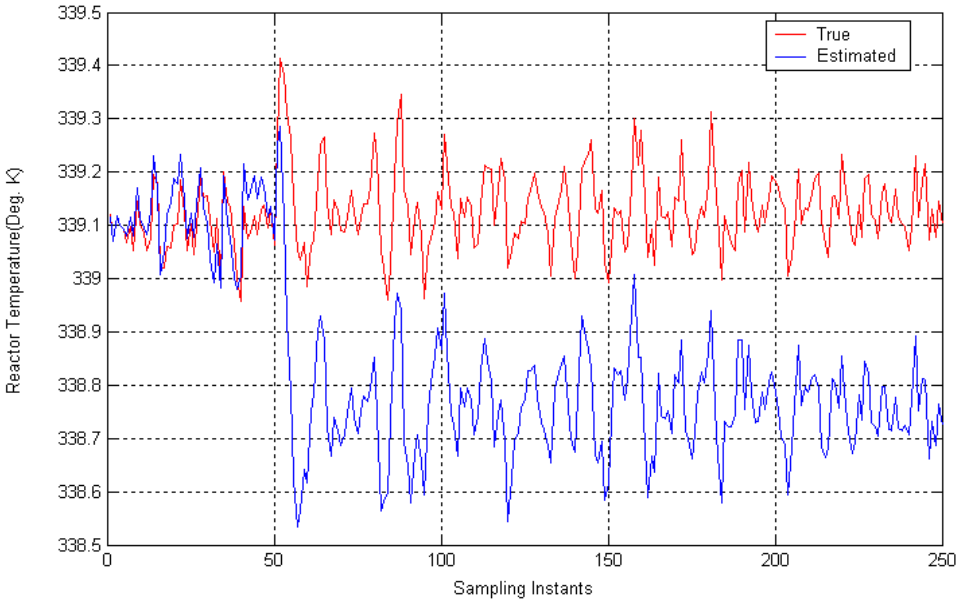

Figure 5.35 Evolution of true and estimated states of reactor temperature of CSTR-II in the presence of step change in feed temperature (FKF based NMPC)

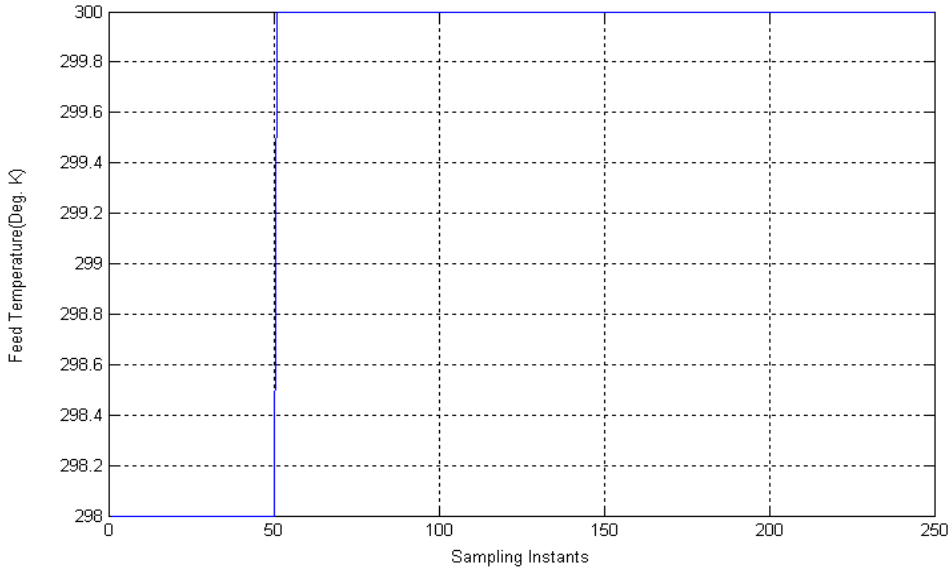

Figure 5.36 Variation in Feed temperature of CSTR-II

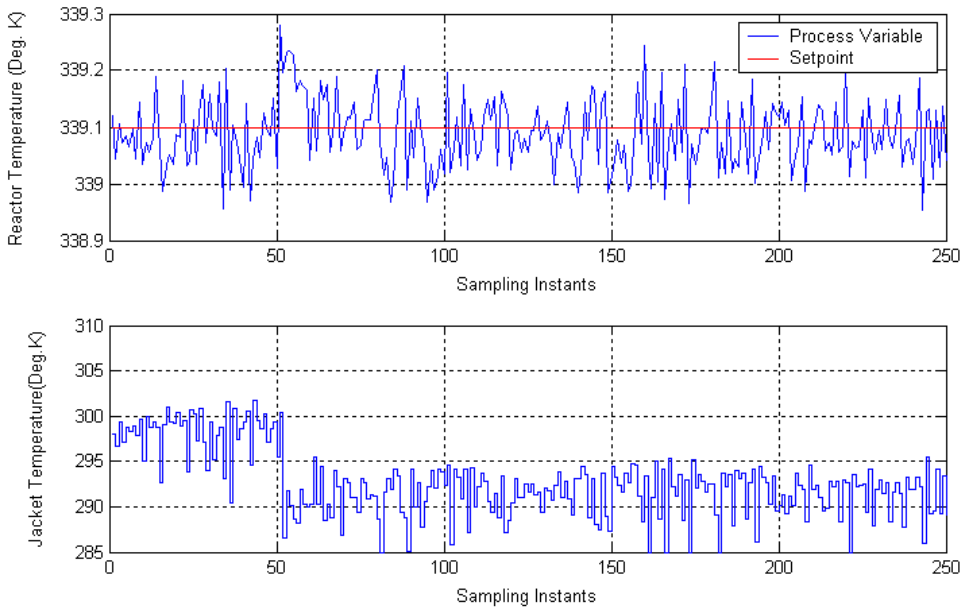

Figure 5.37 Regulatory response of CSTR-II with ASFKF based NMPC (a) Process output (b) Controller output

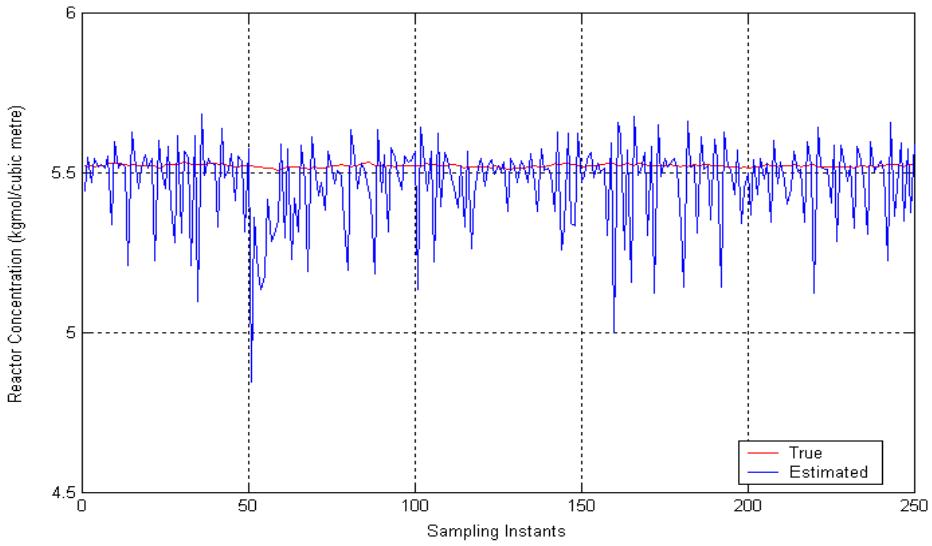

Figure 5.38 Evolution of true and estimated states of reactor concentration of CSTR-II in the presence of step change in feed temperature (ASFKF based NMPC)

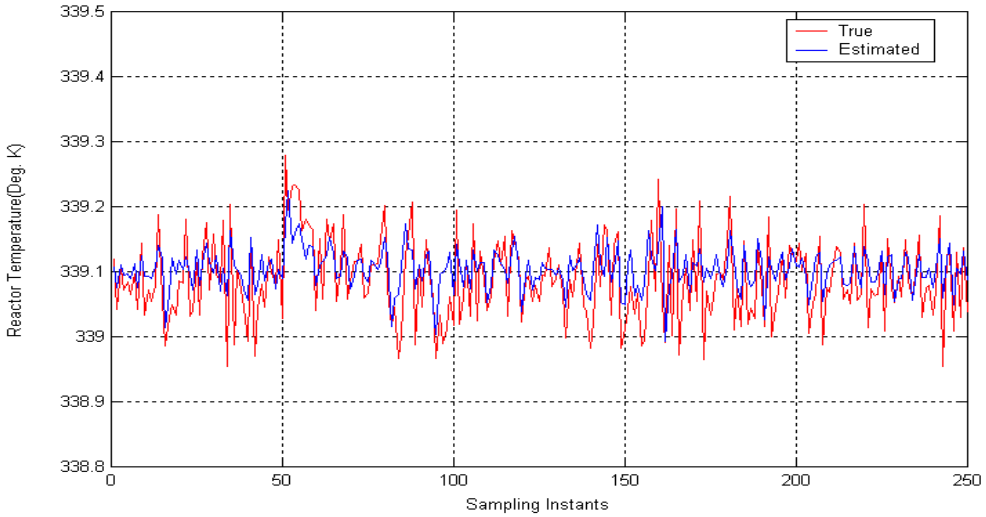

Figure 5.39 Evolution of true and estimated states of reactor temperature of CSTR-II in the presence of step change in feed temperature (ASFKF based NMPC)

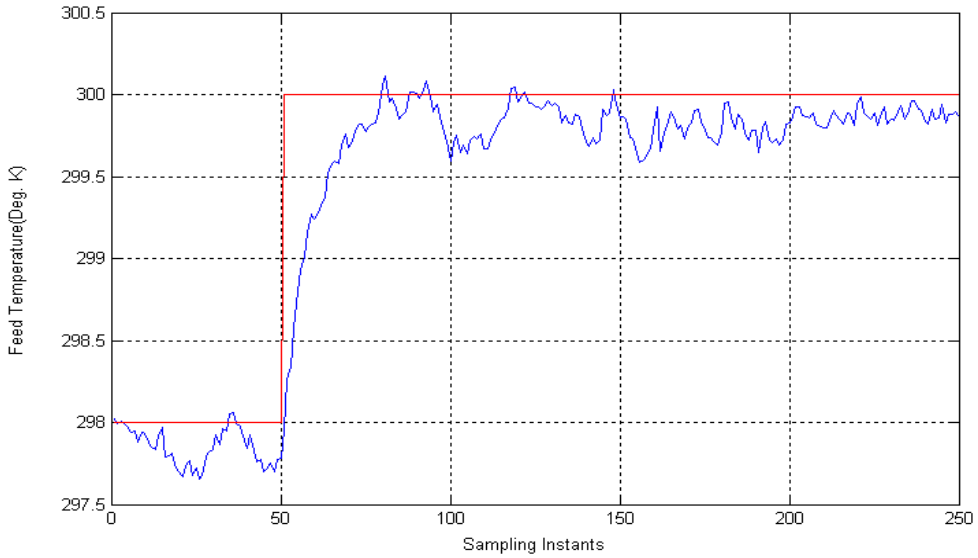

Figure 5.40 Evolution of true and estimated feed temperatures of CSTR-II (ASFKF based NMPC)